Since January 2020 Elsevier has created a COVID-19 resource centre with free information in English and Mandarin on the novel coronavirus COVID-19. The COVID-19 resource centre is hosted on Elsevier Connect, the company's public news and information website.

Journal of Functional Foods 40 (2018) 447–454

Contents lists available at ScienceDirect

Journal of Functional Foods

journal homepage: www.elsevier.com/locate/jff

Mixing ratio optimization for functional complex extracts of *Rhodiola crenulata*, *Panax quinquefolius*, and *Astragalus membranaceus* using mixture design and verification of immune functional efficacy in animal models

Hee-Do Hong, Jong-Chan Kim, Tae-Gyu Lim, Young-Ran Song, Chang-Won Cho, Mi Jang*

Korea Food Research Institute, Iseo-myeon, Wanju-gun, Jeollabuk-do 55365, Republic of Korea

ARTICLE INFO

Keywords:
Optimum mixing ratio
Immune-enhancing activity
Astragalus membranaceus
Panax quinquefolius
Rhodiola crenulata
Functional foods

ABSTRACT

We aimed to identify the optimum mixing ratio for various ingredients to obtain complex extracts with high extract yields and immune-enhancing activity in animals. The extract yield and amounts of nitric oxide (NO) and interleukin (IL)-6 were set to maximum for modeling predictions. The predicted optimum values for the mixing ratio were 49.5% for *Rhodiola crenulata*, 26.1% for *Astragalus membranaceus*, and 24.4% for *Panax quinquefolius*, and the predicted response values were 31.5% yield, 13.4% NO production, and 6.1% IL-6 production; actual values were 35.3% yield, 14.7% NO, and 6.6% IL-6. The optimum mixing ratio extract (OMRE) was used for the animal experiments. Treating mice with OMRE at 200 mg/kg produced significant increases in spleen indexes and T-cell/B-cell proliferation. OMRE treatment increased IL-10 and IL-6 production in concanavalin A- and lipopolysaccharide-induced T- and B- lymphocytes, respectively. These results provide a basis for the development of functional extracts and drinks.

1. Introduction

Recent advances in medicine and science have led to the homo-hundred era, in which excess environmental and industrial advancements have exposed people to viral infections, such as Middle East respiratory syndrome, and harmful environments, such as fine dust. Therefore, there is growing interest in the development of drugs, drinks, and functional foods using natural substances with few side effects (Eliott, 1996). As an essential element in the healthy lifestyle of modern individuals, the importance of immunity has been recognized; accordingly, there has been a recent increase in the consumption of health functional foods that assist in enhancing immunity.

Rhodiola crenulata, which is found in the alpine regions of Northeast Asia, Central Asia, North America, and Northern Europe, is a perennial herb of Angiospermae order, Crassulaceae family, and *Rhodiola* genus, and its roots and stems are used as medicines. In Europe and Asia, *R. crenulata* is a traditional drug with efficacy in stimulating the nervous system, reducing depression, enhancing work capacity, promoting fatigue recovery, and preventing altitude sickness (Ishaque, Shamseer, Bukutu, & Vohra, 2012; Kelly, 2001; Lee, 1998). Unofficially, *R. crenulata* has been used as a fever reducer, sedative, and astringent and has been reported to show antioxidant, anti-inflammatory, antidiabetic, and liver toxicity protection activities (Choe et al., 2012; Kwon, Jang, & Shetty, 2006; Wu, Lian, Jiang, & Nan, 2009; Zou et al., 2015). Recently, researchers have reported that *R. crenulata* has additional beneficial effects, including antioxidant activity (Kanupriya et al., 2005) and protection against neuron damage (Mook-Jung et al., 2002). The main components mediating these effects are salidroside and tyrosol.

Panax quinquefolius is known to have various pharmacological properties, including effects in the cardiovascular and central nervous systems as well as antidiabetic, antitumor, and immunoregulatory effects. Accordingly, *P quinquefolius* is one of the most commonly consumed herbs in the United States of America and is widely used as a commercial material for ginseng products (Ang-Lee, Moss, & Yuan, 2001; Attele, Wu, & Yuan, 1999; Court, 2000).

Astragalus membranaceus is a representative drug used to sustain energy and is known to have several important properties, including warmth, sweetness, and lack of toxins. In oriental medicine, *A. membranaceus* is used to enhance brain function, improve diuresis, increase strength, and prevent gastrointestinal cancers and has been reported to have anti-inflammatory, strength-enhancing, blood glucose level-reducing, immune-enhancing, antitumor, and blood pressure-reducing

Abbreviations: FBS, fetal bovine serum; NO, nitric oxide; IL, interleukin; OMRE, optimum mixing ratio extract; OD, optical density; ELISA, enzyme-linked immunosorbent assay; LPS, lipopolysaccharide

* Corresponding author.
E-mail addresses: honghd@kfri.re.kr (H.-D. Hong), jckim@kfri.re.kr (J.-C. Kim), tglim83@kfri.re.kr (T.-G. Lim), Song.Young-ran@kfri.re.kr (Y.-R. Song), cwcho@kfri.re.kr (C.-W. Cho), jangmi@kfri.re.kr (M. Jang).

https://doi.org/10.1016/j.jff.2017.11.038
Received 28 July 2017; Received in revised form 23 November 2017; Accepted 25 November 2017
Available online 28 November 2017
1756-4646/

effects in pharmacological experiments (Auyeung, Han, & Ko, 2016; Jia, Jiang, Qiao, & Chen, 2003; Shao et al., 2004).

Herbal and oriental medicines consist of many medicinal herbs, in contrast to synthetic drugs, and many substances interact to exhibit medicinal effects. The most notable examples include gumiganghwaltang (Kim et al., 2005; Moon, Go, & Park, 1999), which is used to treat cold and infections, and Sipjjeondaebotang, which is used to treat weak blood flow and cold sweat (Oh et al., 2014). In products with more than one substance, it is difficult to optimize the appropriate component ratios during mixture experiments because the substances often bind to each other to produce independent effects or interact to form a single product. The mixture design method is an experiment used to identify substances that exhibit significant effects on the targeted dependent variable and results in maximum or minimum reaction in mixture extract experiments; this method is also commonly used to determine the optimum mixing ratio (Cornell, 1990).

In this study, we used the mixture design method for functional extract development to identify the optimum mixing ratio of these three commonly used herbs in order to enhance extract yield and immune activity. We then verified the predictions and evaluated the immune-enhancing effects of the optimum mixture extract in an animal model.

2. Materials and methods

2.1. Materials

A. crenulata, *P. quinquefolia*, and *A. membranaceus* were provided by Dalian University, China in April 2016. The samples were pulverized with a grinder, followed by filtration through 60 mesh.

2.2. Experimental design for optimization of the mixing ratio

Planning, data analysis, and optimization were conducted using MINITAB 17 software (Minitab Inc., State College, PA, USA), and the mixture design was the simplex centroid design. Independent variables were *R. crenulata*, *A. membranaceus*, and *P. quinquefolia*, and 10 experimental points at the axis and centroids were set. The extract yield and amounts of nitric oxide (NO) and interleukin (IL)-6 produced by macrophages were measured for each extract. Activated macrophages, T lymphocytes, and NK cells mainly produce cytokines such as TNF-α, IL-6, and IL-1β, and they play important roles in the cellular immune process by promoting the elimination of abnormal cells (Liu et al., 2009). Therefore, NO or IL-6 were considered as the dependent variables of extracts from 10 experimental points in this study. The mixing ratio of the experimental points is shown in Table 1, and all experimental orders were conducted at random to reduce error from division.

2.3. Extraction at 10 experimental points

R. crenulata, *A. membranaceus*, and *P. quinquefolia* were mixed at different ratios based on the design condition (Table 1) and subjected to hot water extraction using distilled water in a 60 °C shaking incubator for 24 h. Each extract was centrifuged (6500*g*, 10 min, 4 °C), and the obtained supernatant was filtered and freeze-dried. The optimum mixing ratio extract (OMRE) produced by mixture design was used for the animal experiments.

2.4. Cell culture

RAW 264.7 murine macrophages were purchased from the Korean Cell Line Bank (KCLB, Seoul, Korea) and cultured in Dulbecco's modified Eagle's medium supplemented with 10% fetal bovine serum (FBS), penicillin (100 U/mL), and streptomycin sulfate (100 μg/mL) at 37 °C in a humidified incubator (5% CO_2).

Table 1
Matrix of the simple centroid mixture design and experiment data of extraction yield, NO production and IL-6 production.

Run	Independent variables[a]			Response variables[b]		
	X_1	X_2	X_3	Y_1[c]	Y_2[c]	Y_3[c]
1	1.00	0.00	0.00	26.7 ± 0.5	33.3 ± 1.4	22.3 ± 0.5
2	0.00	1.00	0.00	47.3 ± 0.1	2.2 ± 0.7	0.8 ± 0.2
3	0.00	0.00	1.00	56.6 ± 1.1	3.8 ± 0.5	1.0 ± 0.3
4	0.50	0.50	0.00	33.5 ± 0.1	21.8 ± 1.2	8.7 ± 1.1
5	0.50	0.00	0.50	30.3 ± 0.1	9.6 ± 0.4	4.4 ± 0.6
6	0.00	0.50	0.50	51.7 ± 0.4	2.4 ± 0.6	0.7 ± 0.1
7	0.33	0.33	0.33	35.4 ± 0.1	2.9 ± 0.7	1.4 ± 0.4
8	0.67	0.17	0.17	28.5 ± 0.1	25.2 ± 1.1	11.8 ± 0.3
9	0.17	0.67	0.17	41.8 ± 0.2	1.2 ± 0.4	0.8 ± 0.2
10	0.17	0.17	0.67	44.0 ± 0.6	1.0 ± 0.2	1.4 ± 0.5

[a] Independent variables: X_1, *Rhodiola crenulata*; X_2, *Panax quinquefolius*; X_3, *Astragalus membranaceus*.
[b] Response variables: Y_1, extraction yield; Y_2, the percentage of NO production in the LPS-induced control; Y_3, the percentage of IL-6 production in the LPS-induced control
[c] All values are mean ± SD of triplicate determinations.

2.5. Measurement of NO

The presence of nitrite, a stable oxidized product of NO, was determined in cell culture medium using Griess reagent. RAW 264.7 macrophages (1×10^5 cells/mL) were cultured in 24-well plates and stimulated with extracts from 10 experimental points (at a concentration 200 μg/mL) for 24 h. One hundred microliters of culture supernatant was collected and mixed with an equal volume of Griess reagent (0.1% N-[1-naphthyl] ethylenediamine dihydrochloride, 1% sulfanilamide, and 2.5% H_3PO_4). After incubation for 15 min, the optical density (OD) was measured at 540 nm using a microplate reader. Nitrite concentrations in the supernatants were determined by comparison with a sodium nitrite standard curve. NO production by 10 extracts from cells treated with different mixing ratios is presented as the percentage of NO production in the lipopolysaccharide (LPS)-induced control.

2.6. Determination of IL-6 production

RAW 264.7 macrophages (1×10^5 cells/mL) were cultured in 24-well plates and stimulated with extracts from 10 experimental points (at a concentration 200 μg/mL). Supernatants were collected after 24 h, and IL-6 levels were determined using a mouse IL-6 enzyme-linked immunosorbent assay (ELISA) kit (BD OptEIA; BD Biosciences Pharmingen, San Diego, CA, USA) according to the manufacturer's protocols. IL-6 production by 10 extracts from cells treated with different mixing ratios is presented as the percentage of IL-6 production in the LPS-induced control.

2.7. Animals and treatments

Male BALB/c mice (8 weeks old) were purchased from the Center of Experimental Animals of Yanbian Medical College of Yanbian University (Yanji, Jilin, China). The mice were kept in microisolator cages and received food and water ad libitum. The laboratory temperature was 24 ± 1 °C, and the relative humidity was 40–60%. Before experimentation, the mice were allowed to adapt to the experimental environment for a minimum of 1 week. All experiments were performed in accordance with the National Institutes of Health (NIH) Guide for the Care and Use of Laboratory Animals. The experimental procedures were approved by the Ethical Committee for the Experimental Use of Animals at Yanbian University (Yanji, Jilin, China). The mice were randomly divided into four groups (10 mice in each group). From days 1 to 30, the four different groups of mice were orally treated the following: control group, saline; OMRE groups, 100 or 200 mg/kg body weight OMRE; and positive control group, 100 mg/kg body weight CVT-E002

(an immunostimulatory polysaccharide-rich extract of the root of North American ginseng [*P. quinquefolius*]) (Biondo, Goruk, Ruth, O'Connell, & Field, 2008), daily. At 24 h after the last administration, mice were weighed and sacrificed by cervical dislocation. The spleens were immediately removed and weighed. The spleen index was calculated as the spleen weight divided by the body weight. Spleen samples were used for splenocyte proliferation.

2.8. Splenocyte proliferation assay and cytokine measurements

Spleens were washed with RPMI 1640 medium and passed through a 200-mesh stainless steel sieve to obtain a homogeneous cell suspension. The spleen cell suspension was washed twice with RPMI 1640-FBS (containing 10% FBS), and the recovered spleen cells were resuspended in Tris-buffered ammonium chloride solution (NH_4Cl, pH 7.2) for 5 min to remove erythrocytes. After centrifugation, harvested spleen cells were resuspended in RPMI 1640-FBS, and the cell numbers were measured with a hemocytometer using trypan blue dye exclusion. Spleen cells were seeded in 96-well plates (3.0×10^5 cells/well) for cell proliferation assays with mitogens, concanavalin A (Con A; 5 μg/mL), or LPS (10 μg/mL), respectively. After incubation, 3-(4,5-dimethylthiazol-2-yl)-2,5-diphenyltetrazolium bromide (0.5 mg/mL) was added to each well, and plates were incubated for 4 h, after which dimethylsulfoxide solution was added to resolve formazan. The absorbance was measured in a microplate reader (Molecular Devices, Sunnyvale, CA, USA) at 540 nm. IL-6 and IL-10 levels in mitogen-induced T- or B-lymphocyte culture media were quantified using ELISA kits, according to the manufacturer's instructions (R&D Systems, Minneapolis, MN, USA).

2.9. Mouse T-cell purification and stimulation for proliferation

Total T cells were isolated from cell suspensions of ground mice spleens by negative selection using the Dynabeads® Untouched™ mouse T cell kit (Invitrogen Life Technologies, Carlsbad, CA, USA). The mouse depletion Dynabeads were washed with isolation buffer (phosphate buffered saline (PBS) containing 0.1% bovine serum albumin (BSA) and 2 mM ethylenediaminetetraacetic acid). Splenocytes were incubated with an antibody mix containing a cocktail of rat IgGs that bind to mouse B cells, NK cells, monocytes/macrophages, dendritic cells, erythrocytes, and granulocytes. The splenocytes were washed with isolation buffer and centrifuged at 350*g* for 8 min at 4 °C. After centrifugation, the supernatant was discarded and the pellets were resuspended and incubated with mouse depletion Dynabeads for 15 min at 25 °C with gentle tilting and rotation. T cells were immuno-magnetically separated from the remaining spleen cells using a DynaMag™-15 magnet (Invitrogen Life Technologies). The supernatant was collected as the untouched T cells fraction. Naïve T cells were stimulated with various concentrations of OMRE (50, 100, or 200 μg/mL) and Dynabeads mouse T-activator CD3/CD28 (Invitrogen Life Technologies) in a humidified CO_2 incubator at 37 °C for 72 h. The total number of viable cells was determined using the CellTiter 96® aqueous non-radioactive cell proliferation assay (Promega, UK). IL-2 and INF-γ levels in activated T cell culture media were quantified using ELISA kits according to the manufacturer's instructions (R & D Systems, Minneapolis, MN, USA).

2.10. High-performance liquid chromatography (HPLC) analysis

Various concentrations of salidroside, ginsenoside Rb_1, and formonetin were used as standard indices to appraise the quality of *Rhodiola crenulata*, *Panax quinquefolius* L., and *Astragalus membranaceus*, respectively (Assinewe, Baum, Gagnon, & Arnason, 2003; Court, Reynolds, & Hendel, 1996; Qin, Lu, Lin, & Ni, 2009; Tian, Yang, Zhang, & Chang, 2010; Wang, You, & Wang, 1992; Wills, Du, & Stuart, 2002; Yoshikawa et al., 1996). Three representative compounds in the extracts from 10 experimental points were identified and quantified by HPLC. The HPLC system consisted of a JASCO PU-2089 pump, JASCO AS-2057 auto injector, and JASCO ultraviolet (UV)-2075 plus Intelligent UV/VIS detector (JASCO Corp., Tokyo, Japan). Data collection and analysis was performed using the Jasco ChromPass chromatography software.

For salidroside, separation was achieved using a Shiseido Capcell PAK C18 column (5 μm, 4.6 mm × 250 mm, Tokyo, Japan) and the column temperature was maintained at 30 °C. The isocratic mobile phase was pumped at a flow rate of 1.0 mL/min, and consisted of freshly prepared 20% methanol filtered through a 0.45 μm filter and degassed by sonication for 15 min prior to use. The injection volume was 20 μL and the detection wavelength was set at 278 nm.

For formononetin, a linear gradient profile was used as follows: water (containing 0.1% phosphoric acid), acetonitrile 97:3 v/v (0–3 min), 97:3–82:18 (3–30 min), and 50:50% (30–60 min) at a flow-rate of 0.8 mL/min. The volume injected was 20 μL. Separation was performed at 35 °C and the detection wavelength was set at 230 nm.

For ginsenoside Rb_1, a comparative analysis was performed using a Waters SunFire C18 column (5 μm, 250 mm × 4.6 mm, Milford, MA, USA) and UV absorption was measured at 203 nm. The mobile phase consisted of solvent I (acetonitrile) and solvent II (water). A gradient procedure was used as follows: 0–20 min, 20–22% I, 80–78% II; 20–45 min, 22–46% I, 78–54% II; 45–50 min, 46–55% I, 54–45% II; 50–55 min, 55–100% I, 45–0% II; 55–60 min, 100–20% I, 0–80% II. The flow rate was maintained at 1.0 mL/min.

For phenolic and flavonoid compounds in OMRE, an analytical HPLC system was employed, which consisted of a JASCO high-performance liquid chromatograph coupled with a UV–visible multi-wavelength detector (MD-910 JASCO). HPLC was operated under the following conditions: YMC-Pack ODS-AM, 250 mm × 4.6 mm, 5 μm column (YMC-Europe, Schermbeck, Germany), column oven temperature 35 °C, and detection at 285 nm. A gradient solvent system consisting of 0.1% acetic acid in water (solvent A) and 0.1% acetic acid in acetonitrile/water (solvent B) was used as follows: 0–1 min, 12% B; 1–18 min, 22% B; 18–28 min, 28% B; 28–35 min, 38% B; 35–48 min, 48% B; 48–54 min, 68% B; 54–60 min, 100% B; 60–67 min, 12%. The flow rate was 1.0 mL/min and the injection volume was 20 μL. The identification of each compound was based on a combination of retention time and spectral matching.

2.11. Statistical analysis

All data are presented as the mean ± standard deviation. Data were analyzed using one-way analysis of variance, followed by Duncan's multiple range test to detect intergroup differences using SPSS software version 20.0 (SPSS Inc., Armonk, NY, USA). Differences with p values of less than 0.05 were considered statistically significant.

3. Results and discussion

3.1. Experimental design for optimizing the ingredient mixing ratio

Experimental points are shown in Fig. 1, and extract yields for 10 extracts with different mixing ratios and amounts of NO and IL-6 produced in RAW 264.7 cells are shown in Table 1. NO and IL-6 production levels for 10 extract mixtures are presented as the percentage of NO and IL-6 production in the LPS-induced control, respectively. The amounts of NO and IL-6 were 1.0–33.3% and 0.7–22.3%, respectively, and the extract yield was 26.7–56.6%.

3.2. Results of regression analysis for the yield of the extract mixture

Regression analysis results of the extract yield using mixture design analysis are shown in Supplementary Table S1. The coefficient of determination (R^2) for the extract yield model was 99.85%, and the adjusted R square (adj R^2) was 99.65%, reflecting the suitability of the

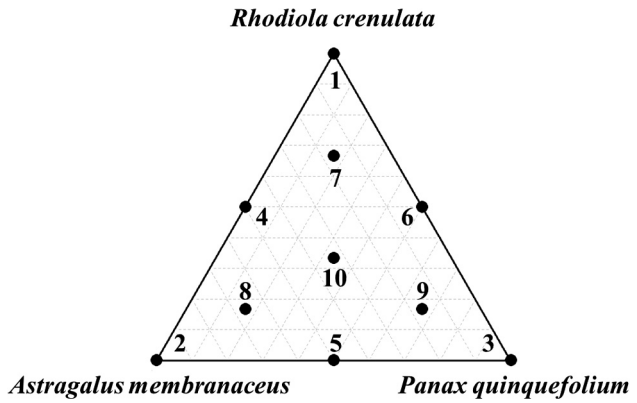

Fig. 1. A simplex centroid design with 10 design points used in the mixture experiment. Basic mixture design for three components representing the three vertices (points 1, 2 and 3), the axial blends (points 4, 5, 6), the centroids of constraint planes (points 7, 8 and 9) and the overall center point (point 10).

model (Supplementary Table S1). The suitability of the model is an essential part of data analysis components, and thus, variance analysis was conducted as shown in Supplementary Table S1 to verify not only the suitability of the reaction model, but also the significance and coefficient of each term (Supplementary Table S1). From interacting terms, *p* values of *R. crenulata* × *A. membranaceus* and *R. crenulata* × *P. quinquefolia* were 0.004 and 0.0001, respectively, reflecting the greatest significance in the reaction model of this experiment. The contour lines for the mixture showed a decreasing trend in yield with an increase in the mixing ratio of *R. crenulata* and in contrast, an increasing trend in the yield with increases in the mixing ratios of *P. quinquefolia* and *A. membranaceus* (Fig. 2A).

3.3. Results of regression analysis for the amounts of NO and IL-6 produced by the extract mixtures

The results of regression analysis for the amount of NO produced using the mixture design analysis are shown in Supplementary Table S2. The R^2 for the NO production model was 92.85%, and the adj R^2 was 83.91%, reflecting the suitability of the model (Supplementary Table S2). The suitability of the model is an essential part of data analysis; thus, variance analysis was conducted as shown in Supplementary Table S2 to verify not only the suitability of the reaction model but also the significance and coefficient of each term. In interacting terms, all *p* values were higher than 0.05 and thus were not statistically significant, reflecting the lack of interaction between independent variables. The contour lines for NO production by mixture showed an increasing trend in the production of NO, an immunologic factor, as the mixing ratio of *R. crenulata* increased, but a decreasing trend in NO production as the mixing ratios of *P. quinquefolia* and *A. membranaceus* increased, suggesting that *A. membranaceus* and *P. quinquefolia* did not greatly affect NO production compared with *R. crenulata* (Fig. 2B). The results of regression analysis for IL-6 production are shown in Supplementary Table S3. The R^2 for the IL-6 production model was 98.61%, and the adj R^2 was 96.87%, reflecting the suitability of the model (Supplementary Table S3). The suitability of the model was further verified with variance analysis as shown in Supplementary Table S3 to verify not only the suitability of the reaction model but also the significance and coefficient of each term (Supplementary Table S3). From interacting terms, the *p* value for *R. crenulata* × *P. quinquefolia* was 0.006, reflecting the greatest significance in the reaction model for this experiment. The contour lines for IL-6 production showed an increasing trend in the production of IL-6, an important cytokine in the immune response, as the mixing ratio of *R. crenulata* increased, but a decreasing trend in IL-6 production as the mixing ratios of *P. quinquefolia* and *A. membranaceus* increased, suggesting that *A. membranaceus* and *P. quinquefolia* did not greatly affect IL-6 production compared with *R. crenulata* (Fig. 2C).

3.4. Optimization of the mixture

It is necessary to determine the optimum mixing ratio for each ingredient to obtain complex extracts with high extraction yields and immune-enhancing activity in order to support the commercial use and economic feasibility of the product. To determine the optimum mixing ratios of *R. crenulata*, *A. membranaceus*, and *P. quinquefolia*, a reaction optimization tool was used in the mixture design. The optimization technique in the mixture design is a method to find the optimum level of factors by gradually moving towards the optimized direction through calculation of response variable values for the experimental point at each stage. By setting extract yields and amounts of NO and IL-6 produced by macrophages to the maximum, the determined reaction equation from the model was used to predict the satisfying numerical point. The predicted optimum values of the mixing ratio to obtain complex extracts with high extract yield, as well as immune enhancing activity, were 49.5% for *R. crenulata*, 26.1% for *A. membranaceus*, and 24.4% for *P. quinquefolia*, and the predicted response values based on the determined mixing ratios were 31.5% yield, 13.4% NO production, and 6.1% IL-6 production (Fig. 3). To verify the predicted response values, extracts, referred to as the OMRE consisting of 50% *R. crenulata*, 26% *A. membranaceus*, and 24% *P. quinquefolia* were prepared, and 35.3% yield, 14.7% NO production, and 6.6% IL-6 production were obtained. In order to identify the substances that significantly affected the response variables and optimum mixing ratios to satisfy the response variables, we used mixture design. Our findings could be used to develop functional drinks with high added value in the food industry. Moreover, *R. crenulata*, which has various physiological activities, could show greater value in improving food quality by mixing *R. crenulata* with *A. membranaceus* and *P. quinquefolia* to develop a complex extract. Recent studies have reported the optimum mixing ratios for *Petasites japonicus*, *Luffa cylindrica*, and *Houttuynia cordata* mixture to treat respiratory diseases (Jeong et al., 2015), and a mixture design has been used to optimizing the mixing ratio in Chinese quince jam production (Lee & Jang, 2009).

3.5. Effects of OMRE on the spleen index and splenic lymphocyte proliferation in mice

The spleen is an important immune organ and is critical for the nonspecific immunity of organisms (Chen, Tang, Wang, Sun, & Liang, 2012). Immune stimulators can increase spleen weights (Chen et al., 2012). Here, mice were treated with the OMRE by oral administration at 100 or 200 mg/kg, and the effects of OMRE on the spleen index are presented in Fig. 4A. When the mice were treated with OMRE at 200 mg/kg, the spleen index was significantly increased compared with that of the control group. The spleen index tended to increase when used at the lower dose as well (100 mg/kg); however, this difference was not statistically significant (Fig. 4A). CVT-E002, an immunostimulatory polysaccharide-rich extract from the roots of North American ginseng (*P. quinquefolium*), was used as a positive control (Biondo et al., 2008). The proliferation of splenic cells is one of the most important steps in the activation of cell-mediated or humoral immunity (Zhao, Li, Luo, & Wu, 2006). Splenic cell proliferation in mice treated with OMRE is presented in Fig. 4B and C. Con A and LPS were used to stimulate T- and B-lymphocyte proliferation, respectively (Cerqueira et al., 2004). T- and B-lymphocyte proliferation was increased in the OMRE-treated group compared with that in the negative control group. Splenic cell proliferation capacity has been widely used as a method to screen for new immune stimulators because cell division and DNA synthesis can be stimulated by various antigens, mitogens, and cytokines (Kruisbeek, Shevach, & Thornton, 2004). In this study, -administration of OMRE increased the mitogen-stimulated proliferation

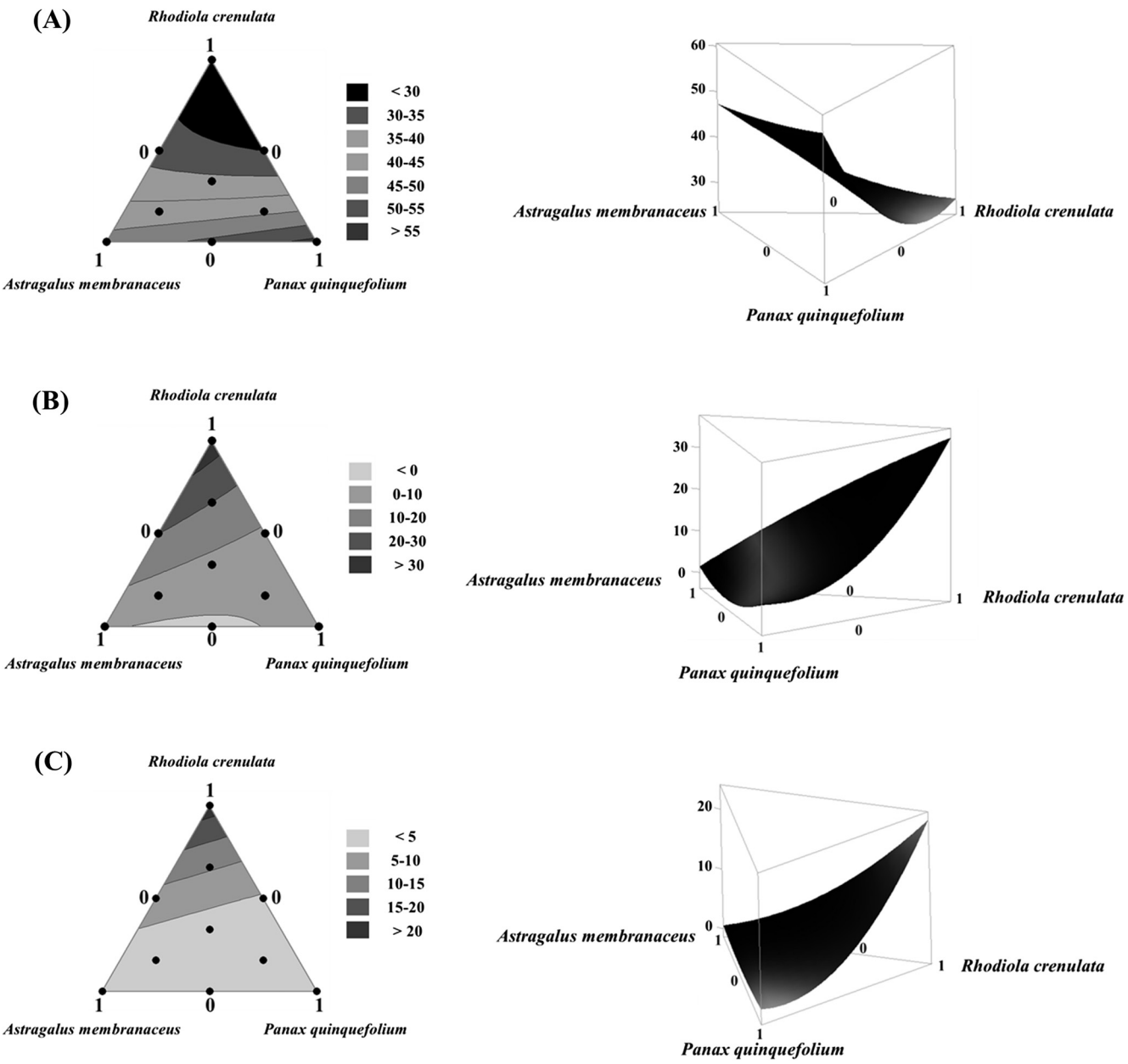

Fig. 2. Mixture contour plots and three-dimensional surface plots showing the interaction effect between three components (*Rhodiola crenulata, Panax quinquefolius, and Astragalus membranaceus*): (A) extraction yield, (B) NO production and (C) IL-6 production. Contour plots are shown on the left and three-dimensional surfaces are shown on the right.

of splenic cells in mice. These results suggested that OMRE activated mouse lymphocytes.

3.6. Cytokine production in mitogen-induced splenocytes

OMRE treatment significantly increased IL-10 cytokine levels in Con A-induced T lymphocytes by stimulation of T cells (Fig. 5A). IL-10 may act in an autocrine manner to suppress antigen-presenting cell (APC) pro-inflammatory responses, act directly on effector T cells to limit their proliferation and function, or promote the differentiation of naive T cells into regulatory populations (Couper, Blount, & Riley, 2008). In LPS-induced B-lymphocyte supernatants, the amount of IL-10 was increased by OMRE treatment (Fig. 5A). Most cytokines with B-cell growth factor activity *in vitro*, including IL-2, IL-4, and IL-10, are also able to induce partial differentiation of B cells into plasma cells secreting Ig (Banchereau & Rousset, 1992). IL-10 is the most potent B-cell differentiation factor, inducing complete differentiation of B cells into mature plasma cells in association with CD40 activation (Rousset et al., 1992). As shown in Fig. 5B, treatment with OMRE at 200 mg/kg significantly increased IL-6 production in Con A- or LPS-stimulated splenocytes supernatants. IL-6 stimulates the terminal differentiation of B cells into plasma cells and plays a central role in fever and acute phase responses (Muraguchi et al., 1988; Sica et al., 1990). IL-6 is secreted by T cells and macrophages to stimulate immune responses and promotes T-cell proliferation, T helper cell differentiation, and T cell-mediated cytotoxicity by CD81 cells. Moreover, IL-6 synergizes with IL-1β in the development of cell-mediated immune responses (Houssiau & Van Snick, 1992; Okada et al., 1988).

3.7. Effects of OMRE on the proliferation and production of IL-2 and IFN-γ in activated mouse T cells

To investigate whether OMRE directly influenced proliferation as well as IL-2 and IFN-γ production, mouse T cells were isolated from spleen by magnetic sorting with Dynabeads and then stimulated with anti-CD3 plus anti-CD28. As shown in Fig. 6A, anti-CD3/CD28 co-

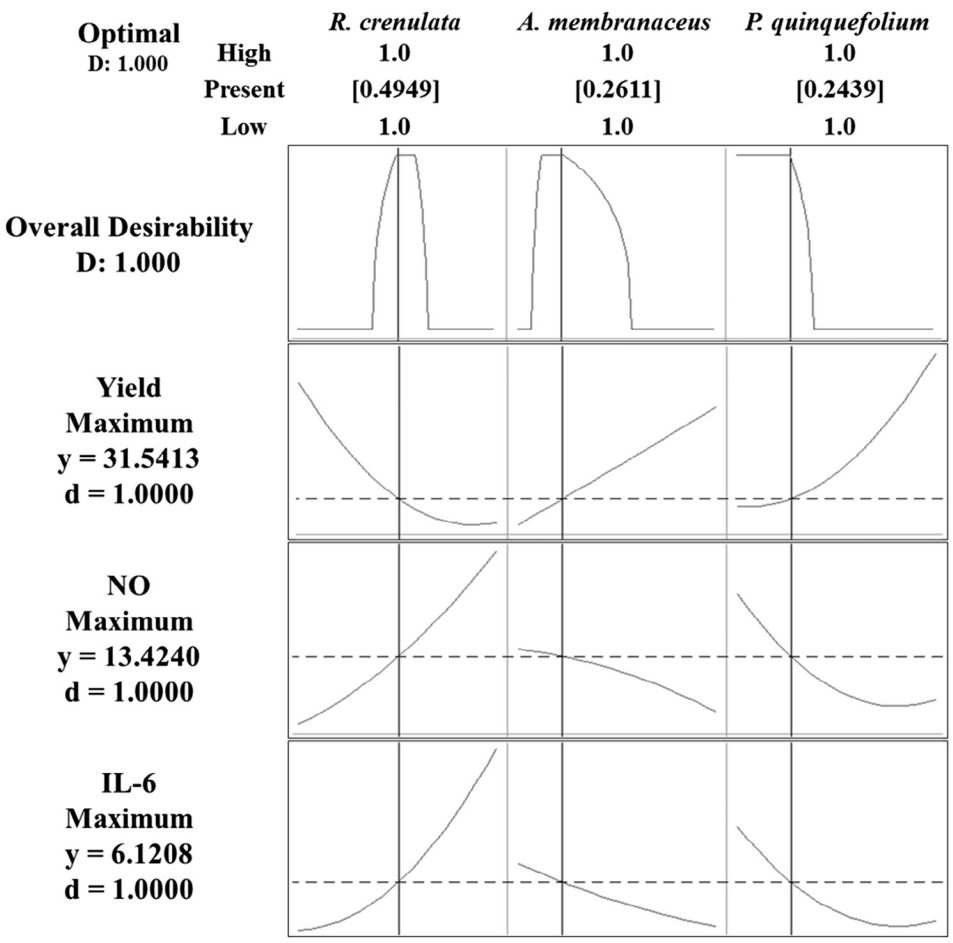

Fig. 3. Mixture design optimization plot for extraction yield, NO production and IL-6 production.

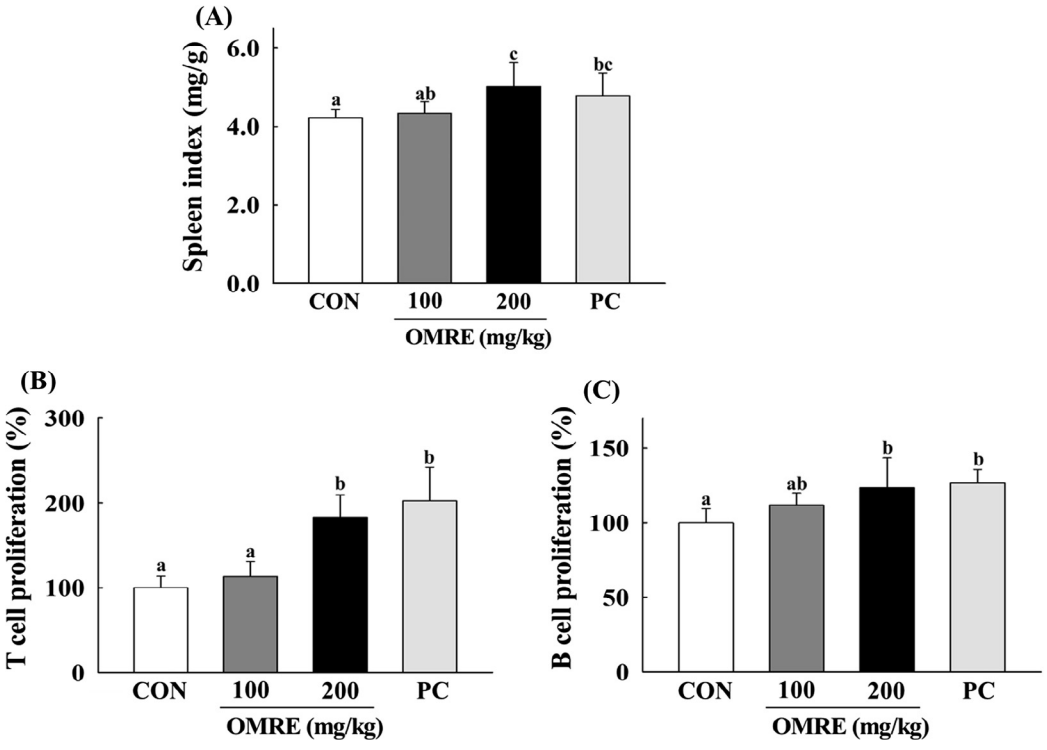

Fig. 4. Effects of OMRE on (A) spleen index, (B) Con A-induced T-lymphocyte and (C) LPS-induced B-lymphocyte proliferations in mice. The data represent the mean ± S.D. (n = 10). CON, saline-treated group; PC, CVT-E002™ (100 mg/kg) treated group (positive control); OMRE, optimum mixing ratio extract-treated group. Values with the different letters are significantly different ($p < .05$).

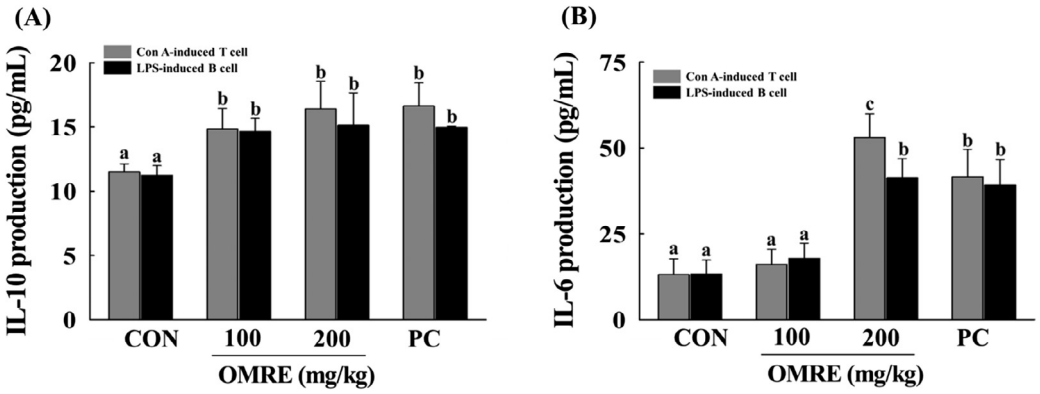

Fig. 5. Effects of OMRE on (A) IL-10 production and (B) IL-6 production in Con A- or LPS-stimulated T- and B-lymphocytes. Data were expressed as mean ± SD. CON, saline-treated group; PC, CVT-E002™ (100 mg/kg) treated group (positive control); OMRE, optimum mixing ratio extract-treated group. Values with the different letters are significantly different ($p < .05$).

stimulation significantly enhanced T-cell proliferation compared to the unstimulated control ($CD3^-/CD28^-$). Proliferation significantly increased when anti-CD3/CD28-activated T cells were treated with OMRE (50, 100, or 200 μg/mL). These results suggest that OMRE enhanced the proliferative capability of anti-CD3/CD28-stimulated T cells. Since OMRE increased the proliferation of anti-CD3/CD28-stimulated T cells, we investigated whether OMRE could affect IL-2 and IFN-γ production in these cells. OMRE significantly increased the production of IL-2 (Fig. 6B) and IFN-γ (Fig. 6C), the hallmark cytokines for Th1-type in anti-CD3/CD28- stimulated T cell.

4. Conclusions

A mixture design method was applied to functional extract development to identify the optimum mixing ratio of these three commonly used herbs in order to enhance extract yield and immune activity. We then verified the predicted optimum values for the mixing ratio and evaluated the immune-enhancing effects of the optimum mixture extract in an animal model. To obtain complex extracts with high extract yield, as well as immune enhancing activity, the predicted optimum values of the mixing ratio were 49.5% for *R. crenulata*, 26.1% for *A. membranaceus*, and 24.4% for *P. quinquefolia*, and the predicted response values were 31.5% yield, 13.4% NO production, and 6.1% IL-6 production. To verify the predicted response values, complex extracts, designated the OMRE, were prepared, consisting of 50% *R. crenulata*, 26% *A. membranaceus*, and 24% *P. quinquefolia*, and 35.3% yield, 14.7% NO production, and 6.6% IL-6 production were obtained. The spleen index and T- and B-lymphocyte proliferation were significantly increased in mice treated with OMRE at 200 mg/kg compared with that of the control group. Treatment with OMRE increased IL-10 and IL-6 production in Con A- or LPS-stimulated T- and B-lymphocytes.

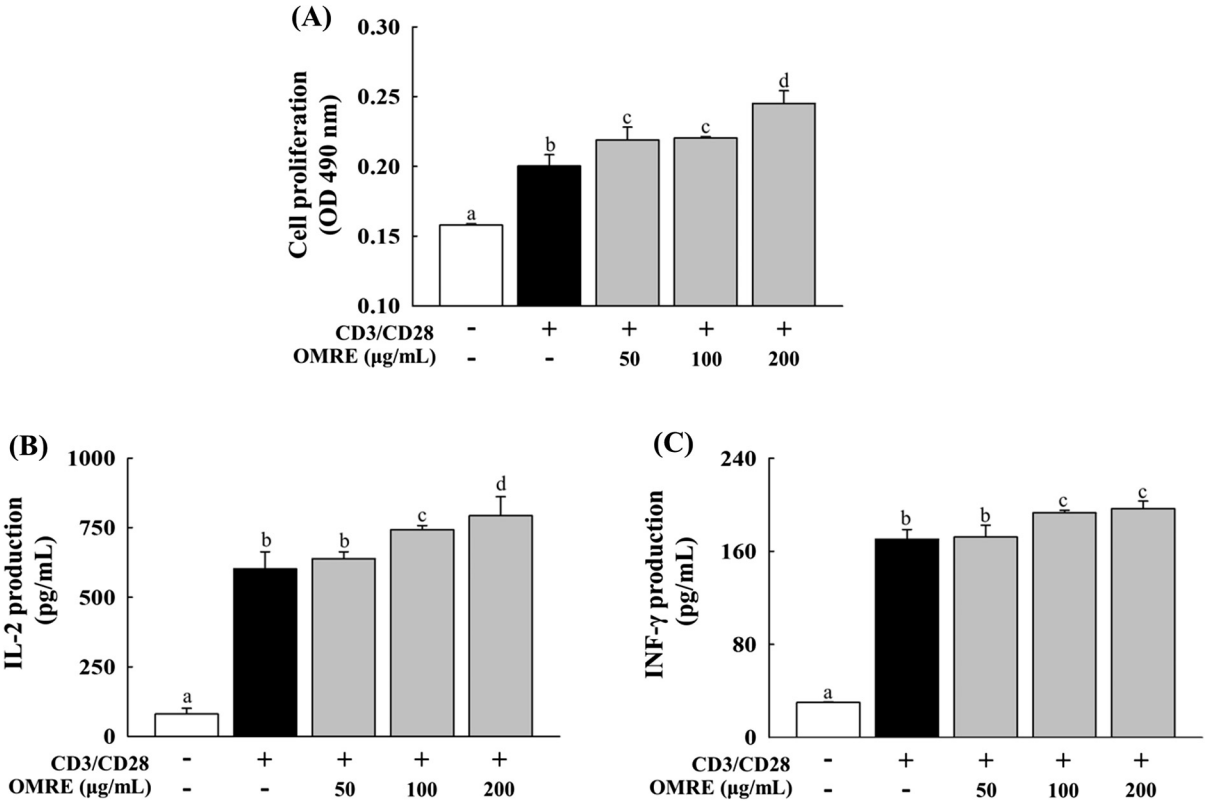

Fig. 6. Effects of OMRE on the proliferation (A), IL-2 production (B), and IFN-γ production (C) in anti-CD3/CD28-stimulated T cells. Data were expressed as mean ± SD. Anti-CD3/CD28-activated T cells were treated with OMRE (50, 100 or 200 μg/mL) for 72 h. Cell proliferation was assessed using the MTS/PMS assay as described in materials and methods. Amounts of IL-2 and IFN-γ were measured by ELISA, respectively. Data were expressed as mean ± SD. Values with the different letters are significantly different ($p < .05$).

Acknowledgements

This research was supported by Main Research Program (ER160502-02) of the Korea Food Research Institute (KFRI) funded by the Ministry of Science, ICT & Future Planning.

Conflict of interest

The authors declare that there are no conflicts of interest.

Appendix A. Supplementary material

Supplementary data associated with this article can be found, in the online version, at http://dx.doi.org/10.1016/j.jff.2017.11.038.

References

Ang-Lee, M. K., Moss, J., & Yuan, C. S. (2001). Herbal medicines and perioperative care. *The Journal of the American Medical Association, 286*, 208–216.

Assinewe, V. A., Baum, B. R., Gagnon, D., & Arnason, J. T. (2003). Phytochemistry of wild populations of *Panax quinquefolius* L. (North American ginseng). *Journal of Agricultural and Food Chemistry, 51*, 4549–4553.

Attele, A. S., Wu, J. A., & Yuan, C. S. (1999). Ginseng pharmacology: Multiple constituents and multiple actions. *Biochemical Pharmacology, 58*, 1685–1693.

Auyeung, K. K., Han, Q. B., & Ko, J. K. (2016). *Astragalus membranaceus*: A review of its protection against inflammation and gastrointestinal cancers. *The American Journal of Chinese Medicine, 44*, 1–22.

Banchereau, J., & Rousset, F. (1992). Human B lymphocytes: Phenotype, proliferation and differentiation. *Advances in Immunology, 52*, 125–262.

Biondo, P. D., Goruk, S., Ruth, M. R., O'Connell, E., & Field, C. J. (2008). Effect of CVT-E002™ (COLD-fX) versus a ginsenoside extract on systemic and gut-associated immune function. *International Immunopharmacology, 8*, 1134–1142.

Cerqueira, F., Cordeiro-Da-Silva, A., Gaspar-Marques, C., Simões, F., Pinto, M. M., & Nascimento, M. S. (2004). Effect of abietane diterpenes from Plectranthus grandidentatus on T- and B-lymphocyte proliferation. *Bioorganic and Medicinal Chemistry, 12*, 217–223.

Chen, X., Nie, W., Fan, S., Zhang, J., Wang, Y., Lu, J., & Jin, L. (2012). A polysaccharide from *Sargassum fusiforme* protects against immunosuppression in cyclophosphamide-treated mice. *Carbohydrate Polymers, 90*, 1114–1119.

Chen, Y., Tang, J., Wang, X., Sun, F., & Liang, S. (2012). An immunostimulatory polysaccharide (SCP-IIa) from the fruit of *Schisandra chinensis* (Turcz.) Baill. *International Journal of Biological Macromolecules, 50*, 844–848.

Choe, K. I., Kwon, J. H., Park, K. H., Oh, M. H., Kim, M. H., Kim, H. H., ... Lee, M. W. (2012). The antioxidant and anti-inflammatory effects of phenolic compounds isolated from the root of *Rhodiola sachalinensis* A. BOR. *Molecules, 17*, 11484–11494.

Cornell, J. A. (1990). *Experiments with mixtures; design, models & the analysis of mixture data*. (2nd ed.). New York: John Wiley & Sons, pp. 24–141.

Couper, K. N., Blount, D. G., & Riley, E. M. (2008). IL-10: the master regulator of immunity to infection. *Journal of Immunology, 180*, 5771–5777.

Court, W. E. (2000). Ginseng: The history of an insignificant plant. *Pharmaceutical Historian, 30*, 38–44.

Court, W. A., Reynolds, L. B., & Hendel, J. G. (1996). Influence of root age on the concentration of ginsenosides of American ginseng (*Panax quinquefolium*). *Canadian Journal of Plant Science, 76*, 853–855.

Eliott, M., Jr. (1996). Biological properties of plant flavonoids: An overview. *International Journal of Pharmacognosy, 34*, 344–348.

Houssiau, F., & Van Snick, J. (1992). IL6 and the T-cell response. *Research in Immunology, 143*, 740–743.

Ishaque, S., Shamseer, L., Bukutu, C., & Vohra, S. (2012). *Rhodiola rosea* for physical and mental fatigue: A systematic review. *BMC Complementary and Alternative Medicine, 12*, 70.

Jeong, H. J., Lee, K. P., Chung, H. S., Kim, D. S., Kim, H. S., Choi, Y. W., ... Lee, Y. G. (2015). Optimization mixture ratio of *Petasites japonicus*, *Luffa cylindrica* and *Houttuynia cordata* to develop a Functional Drink by Mixture Design. *Journal of Life Science, 25*, 329–335.

Jia, R. Z., Jiang, L., Qiao, L. X., & Chen, P. S. (2003). Neuroprotective effects of *Astragulus membranaceus* on hypoxia-ischemia brain damage in neonatal rat hippocampus. *Zhongguo Zhong Yao ZaZzhi, 28*, 1174–1177.

Kanupriya, Prasad, D., Sai Ram, M., Kumar, R., Sawhney, R. C., Sharma, S. K., ... Banerjee, P. K. (2005). Cytoprotective and antioxidant activity of *Rhodiola imbricate* against tert-butyl hydroperoxide induced oxidative injury in U-937 human macrophages. *Molecular and Cellular Biochemistry, 275*, 1–6.

Kelly, G. S. (2001). *Rhodiola rosea*: A possible plant adaptogen. *Alternative Medicine Review, 6*, 293–302.

Kim, S. J., Jeong, H. J., Moon, P. D., Lee, K. M., Lee, H. B., Jung, H. J., ... Kim, H. M. (2005). Anti-inflammatory activity of gumiganghwaltang through the inhibition of nuclear factorkappa B activation in peritoneal macrophages. *Biological and Pharmaceutical Bulletin, 28*, 233–237.

Kruisbeek, A. M., Shevach, E., & Thornton, A. M. (2004). Proliferative assays for T cell function. *Current Protocols in Immunology*, Chapter 3: 3.12.11–3.12.15.

Kwon, Y. I., Jang, H. D., & Shetty, K. (2006). Evaluation of *Rhodiola crenulata* and *Rhodiola rosea* for management of type II diabetes and hypertension. *Asia Pacific Journal of Clinical Nutrition, 15*, 425–432.

Lee, Y. N. (1998). *Flora of Korea* (3rd ed.). Korea: Kyohak Publishing Co277.

Lee, E. Y., & Jang, M. S. (2009). Optimization of Ingredients for the Preparation of Chinese Quince (*Chaenomelis sinensis*) Jam by Mixture Design. *Journal of the Korean Society of Food Science and Nutrition, 38*, 935–945.

Liu, Y., Jiao, F., Qiu, Y., Li, W., Qu, Y., Tian, C., ... Chen, C. (2009). Immunostimulatory properties and enhanced TNF- alpha mediated cellular immunity for tumor therapy by $C_{60}(OH)_{20}$ nanoparticles. *Nanotechnology, 20*, 415102.

Mook Jung, I., Kim, H., Fan, W., Tezuka, Y., Kadota, S., Nishijo, H., & Jung, M. W. (2002). Neurorpotecitve effects of constituents of the oriental crude drugs, *Rhodiola sacra*, *R. sachalinensis* and Tokaku-joki-to, against beta-amyloid toxicity, oxidative stress and apoptosis. *Biological and Pharmaceutical Bulletin, 25*, 1101–1104.

Moon, Y. H., Go, J. J., & Park, J. Y. (1999). The anti-inflammatory and analgesic activities of Gumiganghwaltang. *Korean Journal of Pharmacognosy, 30*, 18–24.

Muraguchi, A., Hirano, T., Tang, B., Matsuda, T., Horii, Y., Nakajima, K., & Kishimoto, T. (1988). The essential role of B cell stimulatory factor 2 (BSF-2/IL-6) for the terminal differentiation of B cells. *The Journal of Experimental Medicine, 167*, 332–344.

Oh, S., Cheon, C., Park, S., Jang, B. H., Park, J. S., Jang, S., ... Ko, S. G. (2014). The analysis of the recent research trend of Sipjeondabo-tang in Korea. *Journal of Society of Preventive Korean Medicine, 18*, 113–123.

Okada, M., Kitahara, M., Kishimoto, S., Matsuda, T., Hirano, T., & Kishimoto, T. (1988). IL-6/BSF-2 functions as a killer helper factor in the in vitro induction of cytotoxic T cells. *Journal of Immunology, 141*, 1543–1549.

Qin, H. P., Lu, J., Lin, R. C., & Ni, K. Y. (2009). Study on isoflavonoids in Radix Astragali. *Chinese Journal of Pharmaceutical Analysis, 29*, 746–751.

Rousset, F., Garcia, E., Defrance, T., Pbronne, C., Vezzio, N., Hsu, D. H., ... Banchereau, J. (1992). Interleukin 10 is a potent growth and differentiation factor for activated human B lymphocytes. *Proceedings of the National Academy of Sciences of the United States of America, 89*, 1890–1893.

Shao, B. M., Xu, W., Dai, H., Tu, P., Li, Z., & Gao, X. M. (2004). A study on the immune receptors for polysaccharides from the roots of *Astragalus membranaceus*, a Chinese medicinal herb. *Biochemical and Biophysical Research Communications, 320*, 1103–1111.

Sica, A., Wang, J. M., Colotta, F., Dejana, E., Mantovani, A., Oppenheim, J. J., ... Matsushima, K. (1990). Monocyte chemotactic and activating factor gene expression induced in endothelial cells by IL-1 and tumor necrosis factor. *Journal of Immunology, 144*, 3034–3038.

Tian, S. Z., Yang, Y. T., Zhang, Z. L., & Chang, L. (2010). Simultaneous determination of calycosin and formononetin in Radix Astragali and its fried product with honey by HPLC. *Chinese Traditional Patent Medicine, 32*, 1365–1368.

Wang, S., You, X. T., & Wang, F. P. (1992). HPLC determination of salidroside in the roots of Rhodiola genus plants. *Yao Xue Xue Bao, 27*, 849–852.

Wills, R. B. H., Du, X. W., & Stuart, D. I. (2002). Changes in ginsenosides in Australian-grown American ginseng plants (*Panax quinquefolium* L.). *Australian Journal of Experimental Agriculture, 42*, 1119–1123.

Wu, Y. L., Lian, L. H., Jiang, Y. Z., & Nan, J. X. (2009). Hepatoprotective effects of salidroside on fulminant hepatic failure induced by D-galactosamine and lipopolysaccharide in mice. *The Journal of Pharmacy and Pharmacology, 61*, 1375–1382.

Yoshikawa, M., Shimada, H., Shimoda, H., Murakami, N., Yamahara, J., & Matsuda, H. (1996). Bioactive constituents of Chinese natural medicines. II. Rhodiolae radix. (1). Chemical structures and antiallergic activity of rhodiocyanosides A and B from the underground part of *Rhodiola quadrifida* (Pall.) Fisch. et Mey. (Crassulaceae). *Chemical and Pharmaceutical Bulletin (Tokyo), 44*, 2086–2091.

Zhao, C., Li, M., Luo, Y., & Wu, W. (2006). Isolation and structural characterization of an immunostimulating polysaccharide from fuzi, *Aconitum carmichaeli*. *Carbohydrate Research, 341*, 485–491.

Zou, H., Liu, X., Han, T., Hu, D., Wang, Y., Yuan, Y., ... Liu, Z. P. (2015). Salidroside Protects against cadmium-induced hepatotoxicity in rats via GJIC and MAPK pathways. *PLoS ONE, 10*, e0129788.